



HAL
open science

Measurements of atmospheric turbulence with the dual-beamwidth method using the MST radar at Gadanki, India

G. D. Nastrom, P. B. Rao, Venkataraman Sivakumar

► **To cite this version:**

G. D. Nastrom, P. B. Rao, Venkataraman Sivakumar. Measurements of atmospheric turbulence with the dual-beamwidth method using the MST radar at Gadanki, India. *Annales Geophysicae*, 2004, 22 (9), pp.3291-3297. hal-00328976

HAL Id: hal-00328976

<https://hal.science/hal-00328976>

Submitted on 18 Jun 2008

HAL is a multi-disciplinary open access archive for the deposit and dissemination of scientific research documents, whether they are published or not. The documents may come from teaching and research institutions in France or abroad, or from public or private research centers.

L'archive ouverte pluridisciplinaire **HAL**, est destinée au dépôt et à la diffusion de documents scientifiques de niveau recherche, publiés ou non, émanant des établissements d'enseignement et de recherche français ou étrangers, des laboratoires publics ou privés.

Measurements of atmospheric turbulence with the dual-beamwidth method using the MST radar at Gadanki, India

G. D. Nastrom¹, P. B. Rao², and V. Sivakumar³

¹St. Cloud State University, St. Cloud, Minnesota 56379, USA

²National Remote Sensing Agency, Hyderabad 500037 AP, India

³Universite de la Reunion, Cassin-97715 St. Denis-C9, France

Received: 29 August 2003 – Revised: 24 February 2004 – Accepted: 3 March 2004 – Published: 23 September 2004

Part of Special Issue “Equatorial and low latitude aeronomy”

Abstract. A brief experiment was conducted during 24–29 April and 9–10 May 2002, using the MST radar at Gadanki, India, to test the dual-beamwidth method of estimating the turbulence kinetic energy (TKE). Because the beamwidth can be modified on only one polarization at a time at Gadanki, an elliptical beam was used with a modified dual-beamwidth analysis. Estimates of the TKE from the dual-beamwidth method and the traditional method are very similar in regions of light winds ($< \sim 10 \text{ ms}^{-1}$). In regions of stronger wind ($> \sim 15 \text{ ms}^{-1}$) the traditional method often gives $\text{TKE} < 0$ because the beam-broadening correction is greater than the observed spectral width. It is suggested that some of the problems with the traditional method are due to the uncertainty in the effective width of the radar beam. In all regions the modified dual-beamwidth method gives $\text{TKE} > 0$ on the beam parallel to the prevailing wind; on this beam the estimates depend only on the ratio of the beamwidths, which is presumably well-known, and the observed spectral widths. The values of TKE from the dual-beamwidth method are approximately constant with height at $0.2 \text{ m}^2 \text{ s}^{-2}$ from about 5 to 7.5 km during the afternoon during both April and May (all April observations were made between 9:00 and 17:00 local time), and then decrease rapidly to about $0.02 \text{ m}^2 \text{ s}^{-2}$ by about 9 km. The data from May extend over one full diurnal period and the diurnal range of TKE during this period is found to be about 5 dB below about 12 km and from about 15 to 19 km, near the tropopause, with maximum values during local afternoon.

Key words. Meteorology and atmospheric dynamics (instruments and techniques; turbulence; general or miscellaneous)

1 Introduction

The traditional method of estimating atmospheric turbulence kinetic energy (TKE) from spectral widths requires the application of correction factors to the measured spectral widths due to the interaction of the radar beam with the background wind (e.g. Atlas, 1964; Hocking, 1985; Nastrom, 1997). While these correction factors are well known in principle, estimates of them are sometimes larger than the observed spectral widths (Hocking, 1986; Fukao et al., 1994; Kurusaki et al., 1996; Nastrom and Eaton, 1997; Narayana Rao et al., 2001; Nastrom and Tsuda, 2001; Satheesan and Krishna Murthy, 2002), especially during relatively strong winds, which implies relatively large uncertainty in them or in the observed spectral widths, since the true corrections cannot be larger than the observed spectral widths.

The dual-beamwidth method for measuring TKE using spectral widths from Doppler radar was recently introduced by VanZandt et al. (2002). The dual-beamwidth method employs the spectral widths measured simultaneously with two different beamwidths and the ratio of the magnitudes of the beamwidths is used under the assumption that the TKE is the same in the sample volumes viewed by both beamwidths. With the dual beamwidth method it is not necessary to have independent estimates of the correction factors to be used or to know the actual magnitudes of the beamwidths used. The uncertainty of the TKE estimates from the dual-beamwidth method is governed only by the uncertainty of the observed spectral widths, suggesting that this method may provide a standard against which to compare estimates made by other methods.

Of course, the dual-beamwidth method can be used only at a small number of radar sites that have dual-beamwidth capability. For example, VanZandt et al. (2002) used observations taken in special experiments at the highly versatile MU radar in Japan, and Latteck et al. (2003) give results from a special experiment in Norway. A brief experiment designed

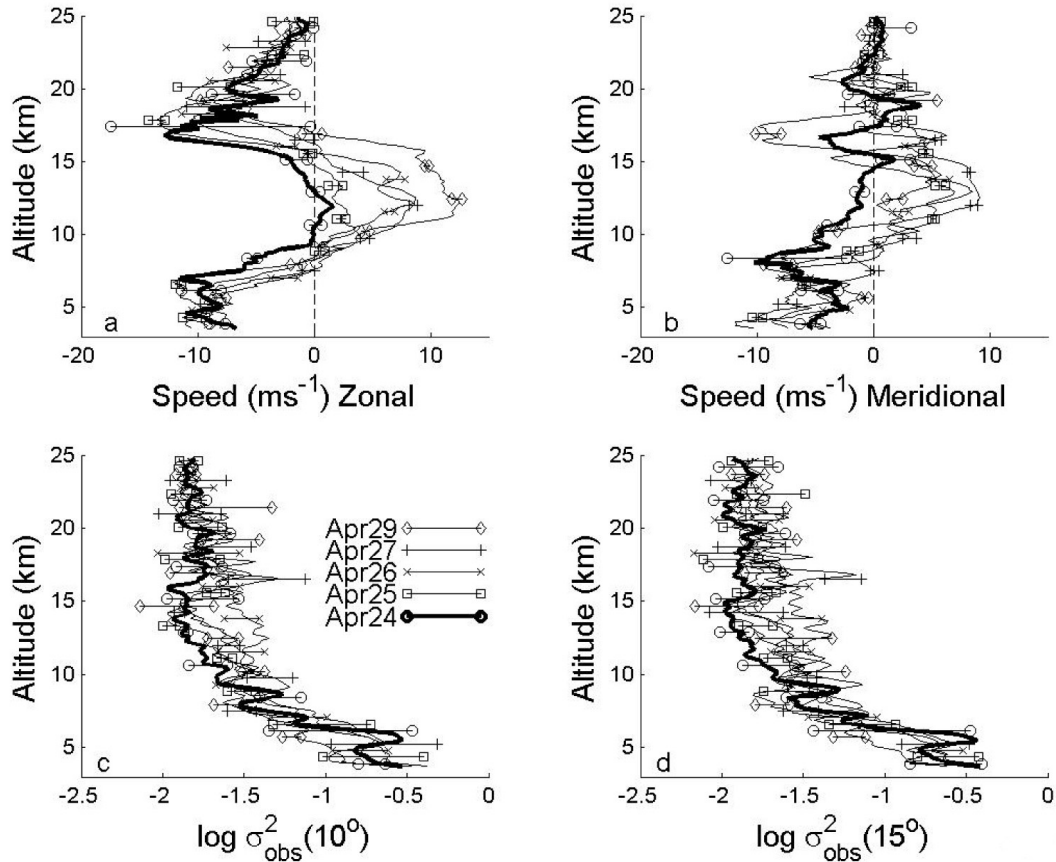


Fig. 1. (Upper) Zonal and meridional wind speeds for each day, April 2002. The plotted curves are the means of the daily medians for the two opposing beams in each plane and for 10° and 15° zenith angle; the symbols show the maximum and minimum values used for each mean. (Lower) Daily means of the observed spectral widths at 10° and 15° zenith angle.

to exercise the dual-beamwidth method was conducted using the MST radar at Gadanki, India, during 24–29 April 2002 and 9–10 May 2002, and the results obtained are described in this paper. Atmospheric conditions over Gadanki, India, are highly repeatable from day-to-day during the pre-monsoon season. Therefore, even the relatively small data sample from this brief pilot study should describe the salient features of the vertical and diurnal variations of TKE for the pre-monsoon conditions.

The estimates of TKE from the traditional method and from a modified dual-beamwidth method are compared in this study. Because the beamwidth of the Gadanki radar could be modified in only one polarization at a time, the dual-beamwidth estimates will be best when the beam is parallel to the prevailing wind, as explained below. Fortunately, during the period used here all of the strong prevailing winds were nearly parallel to the zonal beam.

2 Data

The Gadanki radar is described in detail by others (e.g. Rao et al., 1995; Jain et al., 2000). Briefly, it is an MST radar near Tirupati (13.47° N, 79.18° E) operating at 53 MHz with

average power aperture product of 7×10^8 Wm². The antenna array consists of 1024 crossed 3-element Yagi antennas covering 130×130 m. Peak transmitted power is 2.5 MW obtained from 32 transmitters, each feeding a sub-array of 32 Yagis. The one-way half-power full beamwidth of the full antenna is about 2.9° .

During this experiment two beamwidths were interleaved. The narrow beamwidth (2.9°) was obtained using the full antenna. By disconnecting 16 subarrays from one polarization of the antenna a rectangular antenna was formed, with 2.9° beamwidth in one polarization and a second beamwidth, about 5.8° , in the other polarization. The ratio of the broad and narrow beams is about 2. In practice, the outer 8 subarrays on each side of the antenna were disconnected to form the broad beam. Because the broad beam could be formed only in one polarization at a time, the resulting beam was elliptical (5.8° by 2.9°) and our application of the dual-beamwidth method, described below, will account for this ellipticity.

Our observational strategy included a total of 10 beam positions each hour for each beamwidth: vertical and toward the 4 cardinal directions for 10° and 15° zenith angles. Range-resolution was 150 m from 3.6 to 24.9 km. The radar settings used were: interpulse period, 1000 μ s; number

of incoherent integrations, 128; number of coherent integrations, 1; number of Doppler spectral points, 128; resolution per spectral point, 0.173 ms^{-1} ; dwell-time per profile, 19 s. About 7 profiles were taken per hour per beam per zenith angle per beamwidth. A standard Gaussian fitting method was used to find the Doppler velocity, spectral width, and signal power from each Doppler spectrum. As discussed by Fukao et al. (1994), the uncertainties of the Doppler velocity and spectral width are proportional to the spectral width. Data from the vertical beam are subject to contamination by specular echoes and thus are not used in this study.

Observations were made usually from 11:00–17:00 local time on 24, 25, 26, 27, and 29 April 2002. Another set of observations were taken over a diurnal cycle from 15:00, 9 May–15:00, 10 May 2002. All observations were subjected to a rigorous quality control including visual inspection of the profiles of velocity, signal-to-noise ratio, and spectral width. Finally, hourly medians were formed and are used for the analyses below.

Local weather conditions during late April and early May 2002 were very hot, with daily maximum temperatures near 40°C every day (the Sun is directly overhead at noon at this latitude in late April). Surface winds were generally light and variable. Scattered cumulus and towering cumulus formed in the afternoon, although no significant precipitation occurred at the radar site.

3 Method of analysis

The observed spectral width (σ_{obs}^2) represents the sum of the TKE per unit mass (σ_t^2) and the effects of beam-, shear-, and wave-broadening

$$\sigma_{obs}^2 = \sigma_t^2 + \sigma_{beam+shear}^2 + \sigma_{wave}^2. \quad (1)$$

Nastrom and Eaton (1997) found that in the troposphere σ_{wave}^2 is negligible for radars with short-dwell observations, such as those used here. Following Nastrom (1997), $\sigma_{beam+shear}^2$ can be approximated as

$$\sigma_{beam+shear}^2 = \frac{\theta^2}{4 \ln 2} \left[\left(U^2 \cos^2 \alpha + V^2 \right) - 2Uu_z R \cos \alpha \sin^2 \alpha + (u_z R)^2 \sin^4 \alpha \right], \quad (2)$$

where U and V are the horizontal wind components parallel and perpendicular to the beam, θ is the one-way half-power half-width of the beam, α is the beam zenith angle, $u_z = dU/dz$, and R is the range to the center of the sample volume. Terms of order θ^4 and $(\Delta R/R)^2$ are neglected, where ΔR is the range resolution, a trigonometric identity has been used to obtain $\sin^4 \alpha$, and the vertical component of wind is ignored. In the “traditional method” estimates of σ_t^2 are obtained from Eq. (1) after using the radar observations of wind to compute the right side of Eq. (2), i.e.

$$\sigma_t^2 = \sigma_{obs}^2 - \sigma_{beam+shear}^2. \quad (3)$$

Van Zandt et al. (2002) show that observations of the same sample volume with two conical beams of different beamwidth (θ_a and θ_b) can be used to solve a pair of simultaneous equations to obtain σ_t^2 as a function of σ_{obs-a}^2 , σ_{obs-b}^2 , and the ratio θ_a^2/θ_b^2 , with no need to evaluate Eq. (2) directly.

The beam of the Gadanki radar is conical when the full antenna is used. When only half of the antenna is used for one polarization the beam is elliptical, being 5.8° in the zenith direction and 2.9° azimuthally. Accordingly, our analysis is modified from that of VanZandt et al. (2002). Equation (2) must be written separately for the two beamwidths as follows (subscript H applies for the half-antenna and F for the full-antenna):

$$\sigma_{obs-H}^2 = \sigma_t^2 + \left[\theta_H^2 \left(U^2 \cos^2 \alpha + shear \right) + \theta_F^2 V^2 \right] / 4 \ln 2, \quad (4)$$

$$\sigma_{obs-F}^2 = \sigma_t^2 + \left[\theta_F^2 \left(U^2 \cos^2 \alpha + shear \right) + \theta_F^2 V^2 \right] / 4 \ln 2, \quad (5)$$

where “shear” = $-2Uu_z R \cos \alpha \sin^2 \alpha + (u_z R)^2 \sin^4 \alpha$.

Subtracting Eq. (5) from Eq. (4) gives

$$U^2 \cos^2 \alpha + shear = 4 \ln 2 \left[\frac{\sigma_{obs-H}^2 - \sigma_{obs-F}^2}{(\theta_H^2/\theta_F^2) - 1} \right]. \quad (6)$$

Using Eq. (6) in Eq. (4) gives

$$\sigma_t^2 = \frac{(\theta_H^2/\theta_F^2) \sigma_{obs-F}^2 - \sigma_{obs-H}^2}{(\theta_H^2/\theta_F^2) - 1} - \frac{\theta_F^2 V^2}{4 \ln 2}. \quad (7)$$

The first term on the right of Eq. (7) depends only on the observed spectral widths and the ratio of beamwidths. The second term on the right of Eq. (7) requires that we know θ_F , as well as V . In principle, the width of the transmitted beam is known and that value of θ_F should be used whenever the sample volume is uniformly filled with turbulence. When the sample volume is not filled, such as when one or more thin horizontal layers of intense turbulence are present, then the appropriate value for θ_F depends on the amount of beamfilling, and perhaps other things, and becomes uncertain (e.g. if only a single intense layer is present in the sample volume, then the effective beamwidth is less than θ_F and its value depends on the location of the intense layer within the sample volume). The uncertainty of the value of θ_F may explain why several of the past studies mentioned earlier have obtained results with $\sigma_t^2 < 0$ using the “traditional method”. The dual-beamwidth method, however, is not subject to this problem when V is negligible (i.e. in the beam parallel to the prevailing wind), as long as the ratio θ_H^2/θ_F^2 is constant. A major goal of this study will be to compare estimates of σ_t^2 from Eq. (7) with those from the “traditional method” Eq. (3).

4 Vertical profiles

The upper panels of Fig. 1 show the daily median winds observed at Gadanki during 24–29 April 2002. The plotted

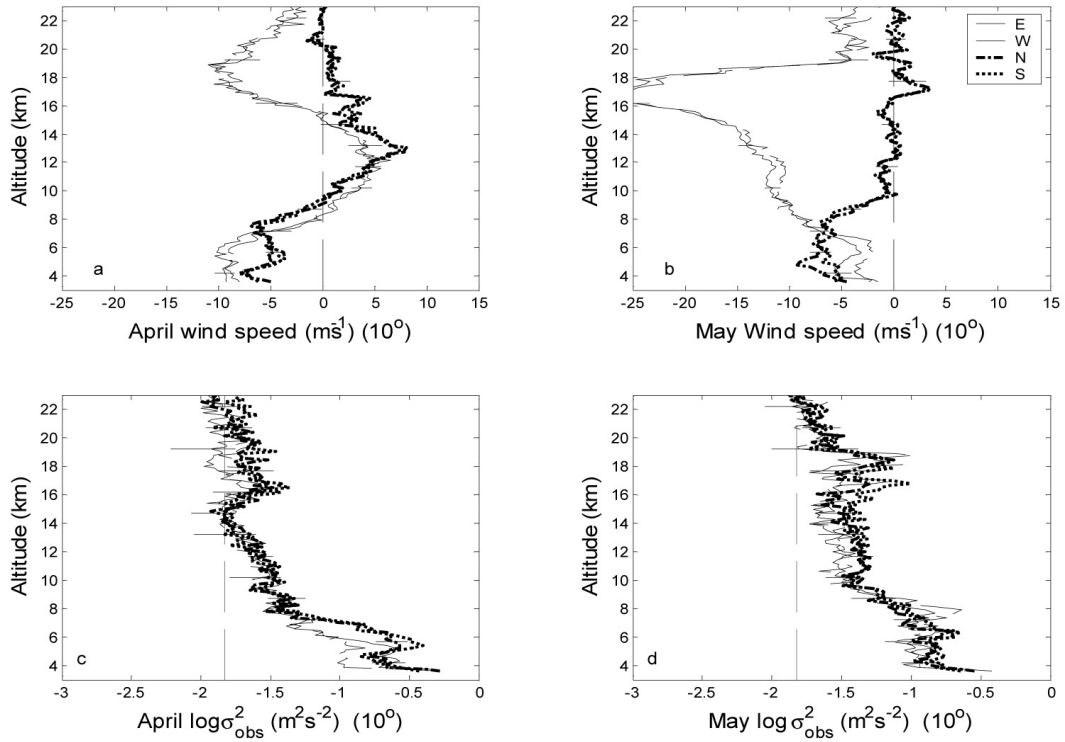


Fig. 2. Median (upper) winds and (lower) observed spectral widths over all observations taken at 10° zenith angle during (left) April and (right) May. Bars extending $\pm 2\sigma/\sqrt{N_o}$ are entered at representative heights along the E and N curves. Dashed vertical lines in the lower panels show the minimum spectral resolution for Doppler half-width.

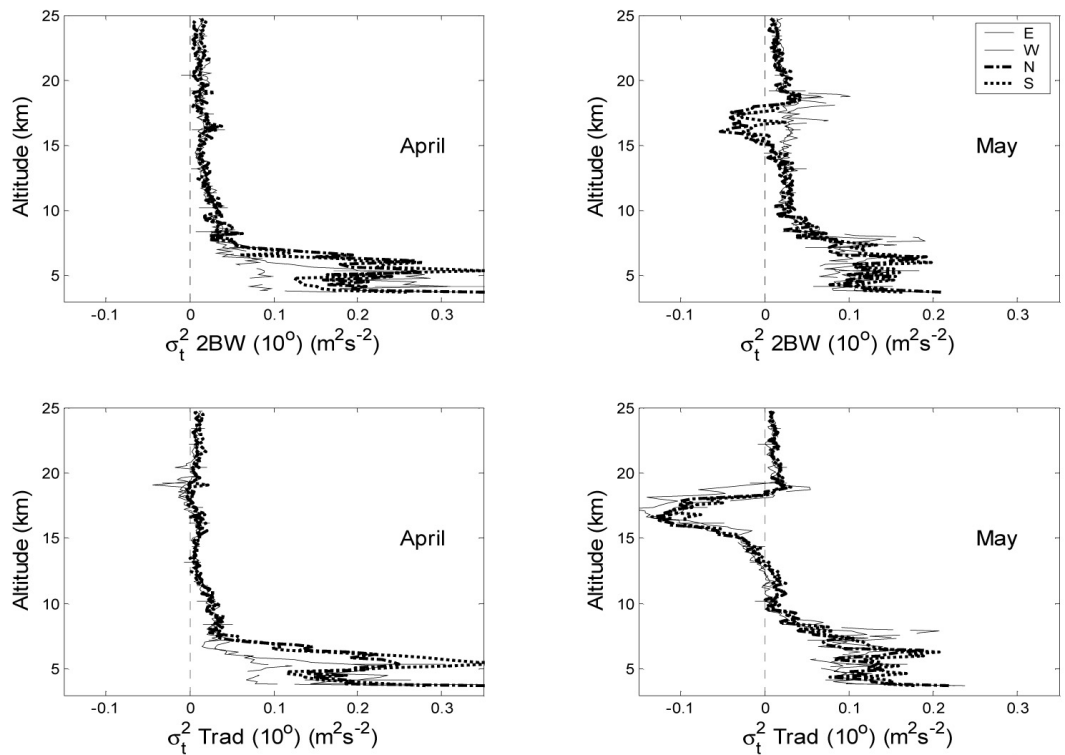


Fig. 3. Median (upper) σ_t^2 -2BW and (lower) σ_t^2 -Trad over all observations taken at 10° zenith angle during (left) April and (right) May. Bars extending $\pm 2\sigma/\sqrt{N_o}$ are entered at representative heights along the E and N curves.

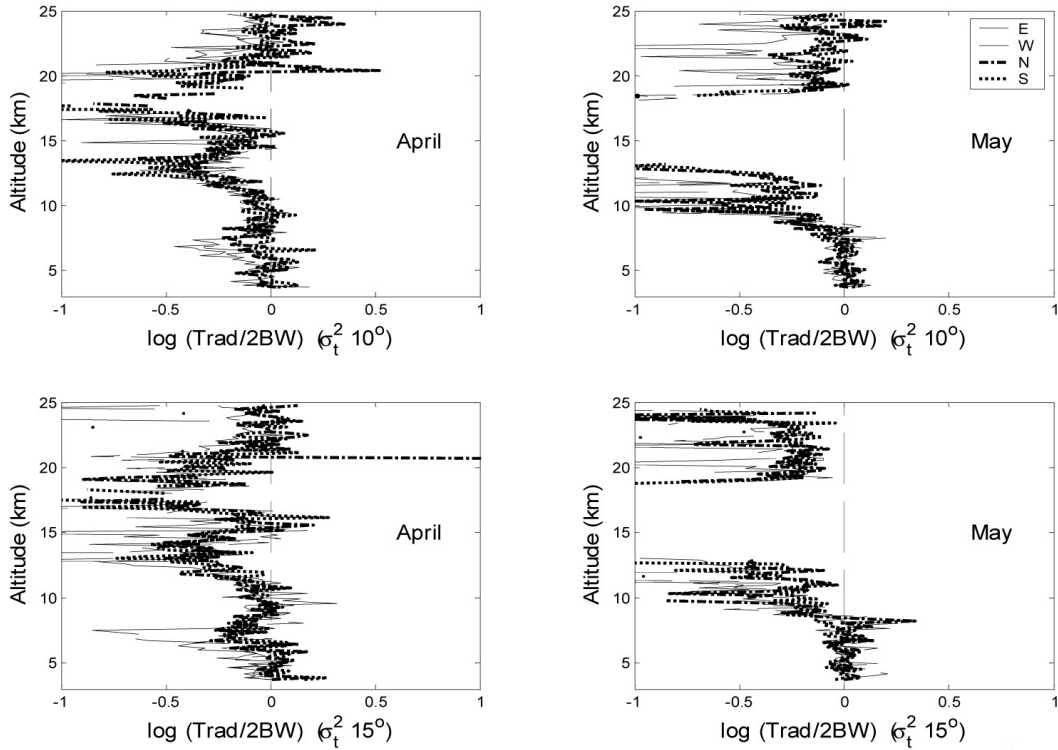


Fig. 4. Ratio of the median σ_t^2 -Trad to the median σ_t^2 -2BW during (left) April and (right) May for observations taken at (upper) 10° and (lower) 15° zenith angles.

curves are the mean of four results for each day: the east and west (north and south) beams and at 10° and 15° zenith angles. The symbols show the maximum and minimum value among the four results; in general there is very little variation between the maximum and minimum for each day; i.e. the differences between winds on opposed beams and at 10° and 15° zenith angles appear to be insignificant, except near about 18 km on some days. The flow is characterized as northeasterly (i.e. southwestward) below about 7 km, southwesterly from about 10–15 km after 24 April and easterly above about 17 km. While the declining signal-to-noise ratio with height leads to greater variability above about 17 km, there appears to be useful wind data at all heights in most cases.

The lower panels of Fig. 1 are similar to the upper panels, except they show the daily mean σ_{obs}^2 . In general, there is no clear pattern of differences among the individual days, except near 12 km, where both wind components are very light on 24 April and the associated σ_{obs}^2 is relatively small. Apparently, the larger wind speeds lead to larger σ_{obs}^2 due to beam broadening and, perhaps, stronger turbulence. Ghosh et al. (2003) also found that for relatively light wind speeds there is not a strong effect of wind speed on σ_{obs}^2 at Gadanki. Because there is relatively little change from day to day, we will combine all days in April together in the analyses to follow.

Figure 2 shows the profiles of median wind speed during the entire period in April (upper left) and in May (upper

right) from the 10° zenith angle observations (results at 15° are nearly identical and are not shown). Both periods show northeasterly winds below about 7 km. Above about 10 km the meridional winds in May are very light while the zonal winds continue to increase with height to a maximum speed near 25 ms^{-1} at 17 km. Above about 20 km winds during the two periods are again very similar. Error bars to show the 95% confidence limits extend \pm one standard error of the mean ($2\sigma/\sqrt{N_o}$, where σ is the standard deviation of the N_o hourly medians used) from the curves for the E and N beams.

The lower panels of Fig. 2 show σ_{obs}^2 during April (lower left) and May (lower right). Except at about 5–7 km and perhaps 17–19 km, where the meridional beams’ values are greater than the zonal beams’, there is no significant difference among σ_{obs}^2 for the four beams during April. During May the meridional beams’ σ_{obs}^2 values slightly exceed the zonal beams’ from about 11–17 km. The dashed vertical lines show the Doppler resolution for spectral width as used here; in April (May) the values near 14 km and above about 19 km (22 km) are near the resolution limit.

The upper panels of Fig. 3 show σ_t^2 estimated using Eq. (7), called σ_t^2 -2BW. The lower panels show σ_t^2 estimated using Eq. (3), called σ_t^2 -Trad. Below about 7 km (8 km) during April (May) results from both methods are relatively large, ranging between about 0.1 and $0.3 \text{ m}^2\text{s}^{-2}$, corresponding to the altitudes of active convection. Values for the west beam are consistently smaller than those from the other beams in April below 6 km; from 6 to 7.5 km values

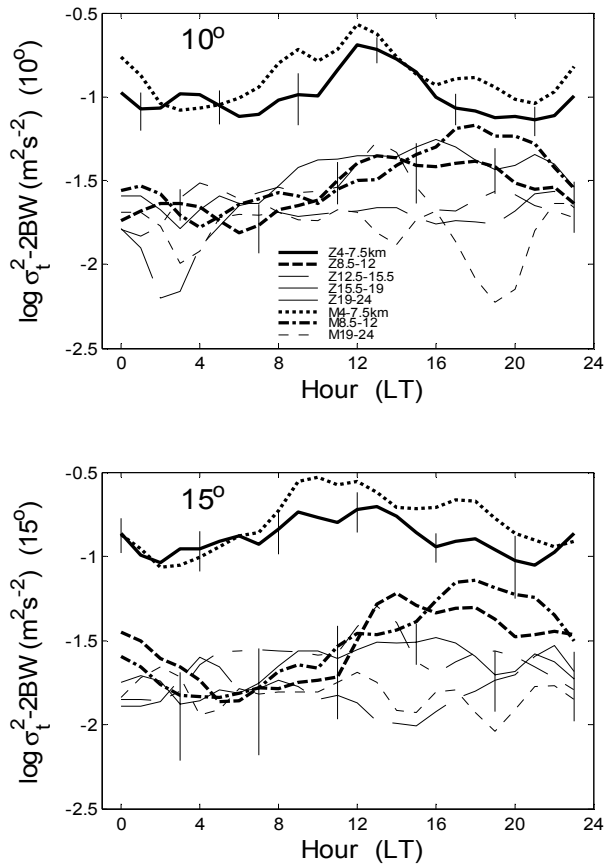


Fig. 5. Hourly medians during 9–10 May of σ_t^2 -2BW over layers in the troposphere and lower stratosphere in the zonal (Z) and meridional (M) planes. Results for the meridional plane at 12–19 km are negative due to strong zonal winds and are not shown. Bars extending $\pm 2\sigma/\sqrt{N_o}$ are entered at representative hours along the Z4–7.5 and Z8.5–12 (Z15.5–19) curves in the upper (lower) panel.

for both beams in the zonal plane are smaller than those in the meridional plane. During May there is no apparent anisotropy at the lower altitudes. Above 7 or 8 km all values become less than $0.02 \text{ m}^2 \text{ s}^{-2}$ at all altitudes except in the regions of strong winds (discussed below); the σ_t^2 -Trad values are slightly smaller than those for σ_t^2 -2BW.

Note that negative values, where the corrections are larger than σ_{obs}^2 , are included in Fig. 3. The May results near 17 km illustrate the differing effects of the correction terms in Eqs. (3) and (7); i.e. for σ_t^2 -Trad the beam-broadening corrections due to the large zonal wind speeds cause values for all four beams to be negative while for σ_t^2 -2BW only the meridional beams' values are negative. A similar, but smaller, effect is seen near 18 km during April. σ_t^2 -2BW may be expected to be more reliable as it is not influenced by thin-layer effects or other beam-filling problems. The curves in Fig. 3 are very similar where the winds are less than about 10 m/s, i.e. except from about 16–19 km during April and 12–19 km during May.

The data above about 20 km appear nearly constant with height. This may reflect the lower bound of σ_t^2 detectable with the Gadanki radar.

Figure 4 compares the σ_t^2 -Trad and σ_t^2 -2BW results for the 10° (15°) zenith angle in the upper (lower) panels. During May the ratios are near unity below about 8 km, corresponding to the altitudes where σ_t^2 appears to be enhanced due to convection (Fig. 3). However, during April the region where the ratios are near unity extends much higher, to over 11 km. Above about 20 km the ratios are again near unity (within 1 or 2 dB), although this may be explained by the spectral widths falling to their minimum detectable signal as noted earlier. There is very little difference between the results at 10° and 15° zenith angle.

5 Diurnal changes

Figure 5 shows the hourly march of σ_t^2 -2BW during 9–10 May for the median values over five vertical layers (4–7.5, 8.5–12, 12–15.5, 15.5–19, and 19–24 km) for beams in the zonal and meridional planes at 10° (15°) in the upper (lower) panel. Results for the meridional beam at 12–19 km are not shown as they are generally negative due to the strong zonal winds in this region. The curves were smoothed with a 1/4-1/2-1/4 filter.

Diurnal changes with ranges of about 5 dB are seen in the layers below 12 km and at 15.5–19 km. The results show very little variation among zenith angles. At 4–7.5 km the maximum (minimum) values occur near local noon (midnight), suggesting the enhanced TKE is related to a daytime process such as convection. At 8.5–12 km and at 15.5–19 km the curves show maxima (minima) in late afternoon (early morning). The latter maxima may be caused by the deeper convection that appears only in the afternoon. Curves at other heights have indistinct diurnal cycles.

Narayana Rao et al. (2001) present a climatology of eddy dissipation rates (ε) at Gadanki based on σ_t^2 -Trad from the radar observations combined with semi-daily radiosonde profiles of the Brunt-Väisälä frequency (N). The diurnal changes in ε that they give must be largely due to changes in σ_t^2 -Trad, since diurnal changes in N are relatively small above the planetary boundary layer. During the season March–May they find the diurnal range of ε (and thus of σ_t^2 -Trad) is about 5 dB in the upper troposphere and lower stratosphere, similar to Fig. 5. However, the time of daily maximum they give is at night, from 22–04 LT, in contrast to the daytime maxima in Fig. 5. We find this difference in time of maximum perplexing and suggest it should be investigated more closely when a larger data set becomes available.

6 Summary and conclusions

A brief experiment was conducted with the MST radar at Gadanki, India, to test the dual-beamwidth method for estimating TKE. Because the antenna size could be changed for only one polarization at a time the resulting beam was elliptical rather than conical. Theoretical analysis showed that in the dual-beamwidth method for an elliptical beam

there is a term that depends on the windspeed perpendicular to the beam (the final term in Eq. 7). During the April period the winds were relatively light at all altitudes, and there was relatively good agreement between results from the dual-beamwidth method and the traditional method. However, during the May period, from about 14 to 18 km, the zonal winds were relatively strong and the meridional winds were nearly calm. Our estimates of TKE during May by the dual-beamwidth method for the zonal beam are positive while those from the meridional beam and from the traditional method are negative, giving a good illustration of the ability of this method to extract TKE during strong winds (at least in the beam parallel to the wind) when the traditional method fails.

The following specific points have been noted:

1. Winds and turbulence from 10° and 15° zenith angles are the same.
2. Winds and turbulence from opposing beams in the same plane are the same.
3. During light wind conditions, σ_t^2 from the modified dual-beamwidth method and the traditional method are the same. During strong wind conditions (over about 15 ms⁻¹) the modified dual-beamwidth method continues to give realistic estimates in the beam parallel to the wind while for the other plane, and for both planes with the traditional method, the corrections are larger than the observed spectral width.
4. Values of σ_t^2 are about 10⁻¹ m²s⁻² in the troposphere (3.6–7.5 km), and about 10⁻² above about 9 km. Values above 12 km are slightly larger during the May period when winds were stronger.
5. The diurnal range of σ_t^2 is about 5 dB below about 12 km. Maximum values occur near local noon at 4.5–7 km and several hours later at 8.5–12 km. The diurnal cycle at 15.5–19 km is very similar to that at 8.5–12 km.

Acknowledgements. G. D. Nastrom was partially supported by the National Science Foundation ATM-0129464 and the Air Force Office of Scientific Research F496200210167.

Topical Editor U.-P. Hoppe thanks S. Cohn and another referee for their help in evaluating this paper.

References

- Atlas, D.: Advances in radar meteorology, edited by Landsberg, H. and van Mieghem, J., Academic, Adv. Geophys., 10, 317–478, 1964.
- Fukao, S., Yamanaka, M. D., Ao, N., Hocking, W. K., Sato, T., Yamamoto, M., Nakamura, T., Tsuda, T., and Kato, S.: Seasonal variability of vertical eddy diffusivity in the middle atmosphere, 1. Three-year observations by the middle and upper atmosphere radar, *J. Geophys. Res.*, 99, 18 973–18 987, 1994.
- Ghosh, A. K., Jain, A. R., and Sivakumar, V.: Simultaneous MST radar and radiosonde measurements at Gadanki (13.5° N, 79.2° E), 2. Determination of various atmospheric turbulence parameters, *Radio Sci.*, 38, (1), 1014, doi:10.1029/2000RS002528, 2003.
- Hocking, W. K.: Measurement of turbulent energy dissipation rates in the middle atmosphere by radar techniques: a review, *Radio Sci.*, 20, 1403–1422, 1985.
- Hocking, W. K.: Observation and measurement of turbulence in the middle atmosphere with a VHF radar, *J. Atmos. Terr. Phys.*, 48, 655–670, 1986.
- Jain, A. R., Narayana Rao, D., and Rao, P. B.: Indian MST radar – An overview of the scientific programmes and results, *Indian J. Radio & Space Phys.*, 29, 149–171, 2000.
- Kurosaki, S., Yamanaka, M. D., Hashiguchi, H., Sato, T., and Fukao, S.: Vertical eddy diffusivity in the lower and middle atmosphere: A climatology based on the MU radar observations during 1986–1992, *J. Atmos. Terr. Phys.*, 58, 727–734, 1996.
- Latteck, R., Singer, W., and Engler, N.: Application of the dual-beamwidth method to a narrow beam MF radar for estimation of spectral width, *Proceedings, MST10 Workshop on technical and scientific aspects of MST radar*, Piura, Peru, 90, 2003.
- Narayana Rao, D., Narayana Rao, T., Venkataratnam, M., Thulasiraman, S., Rao, S. V. B., Srinivasulu, P., and Rao, P. B.: Diurnal and seasonal variability of turbulence parameters observed with Indian mesosphere-stratosphere-troposphere radar, *Radio Sci.*, 36, 1439–1457, 2001.
- Nastrom, G. D.: Doppler radar spectral width broadening due to beamwidth and wind shear, *Ann. Geophys.*, 15, 786–796, 1997.
- Nastrom, G. D. and Eaton, F. D.: Turbulence eddy dissipation rates from radar observations at 5–20 km at White Sands Missile Range, New Mexico, *J. Geophys. Res.*, 102, 19 495–19 506, 1997.
- Nastrom, G. D. and Tsuda, T.: Anisotropy of Doppler spectral parameters in the VHF radar observations at MU and White Sands, *Ann. Geophys.*, 19, 883–888, 2001.
- Rao, P. B., Jain, A. R., Kishore, P., Balamuralidhar, P., Damle, S. H., and Viswanathan, G.: Indian MST radar, 1. System description and sample vector wind measurements in ST mode, *Radio Sci.*, 30, 1125–1138, 1995.
- Satheesan, K. and Krishna Murthy, B. V.: Turbulence parameters in the tropical troposphere and lower stratosphere, *J. Geophys. Res.*, 107, (D1), ACL 2–1, doi:10.1029/2000JD000146, 2002.
- VanZandt, T. E., Nastrom, G. D., Furumoto, J., Tsuda, T., and Clark, W. L.: A Dual-Beamwidth Method for observing atmospheric turbulence intensity with radar, *Geophys. Res. Lett.*, 29, (12), doi:10.1029/2001GL014283, 2002.